Journal of Operation and Automation in Power Engineering

Vol. 7, No. 2, Oct. 2019, Pages: 235-245

http://joape.uma.ac.ir

An Adaptive Load Voltage Support Control Strategy for Inverter-based Renewable Energy Conversion System

M. Shahparasti [1,*], *P. Teimourzadeh Baboli* [2]

[1] *Department of Electrical Engineering, Islamic Azad University, East Tehran Branch, Tehran, Iran.*

[2] *Faculty of Engineering and Technology, University of Mazandaran (UMZ), Babolsar, Iran .*

Abstract- *In this paper, an adaptive load voltage support control strategy is proposed for the inverter to simultaneously control the load voltage, grid current and power injected to the grid in the presence of grid voltage distortions and nonlinearity of the load current. In the proposed control strategy, the local load can be supplied in desired quality of the network operator. In order to employ the proposed control strategy, a cascaded structure has been proposed to control the quality of active injected power to the grid, load voltage and grid current, simultaneously. The proposed controller is able to track and compensate voltage harmonics without need of complex and long-run calculations. The proposed model is simulated under the non-ideal grid conditions while supplying a nonlinear load. The simulation results show the effectiveness of the proposed control strategy to supply a non-linear load in a standard voltage and current.*

Keyword: DC/AC energy conversion, Inverter control in stand-alone mode, Inverter control in grid-connected mode, harmonic compensation, Voltage source inverter.

NOMENCLATURE

C_f	capacitor of LC filter
$G_i(s)$	current controller
$G_v(s)$	voltage controller
g_i	inverter gain
Hf	Harmonic factor
i	inverter current
i_g	current of the grid
i_{load}	load current
i_{gh}	h^{th} harmonic of the grid current
k_{i1}	integral gain
k_{p1}	proportional gain
L	interface inductor
L_f	inductor of LC filter
m	active power controller gain
Hf	harmonic factor
H_i	current feedback gain
H_p	power feedback gain
H_v	voltage feedback gain
$P*$	active power reference
R	equivalent resistance of output load
r	equivalent resistance of interface inductor
THD	Total Harmonic Distortion
V	phase to neutral voltage of the load
V^*	voltage reference
V_g	phase to neutral voltage of the grid
V_i	output voltage of inverter bridge
V_h	h^{th} harmonic of the load voltage
V_{gh}	h^{th} harmonic of the grid voltage
ω	grid frequency
δ	phase angle of the reference voltage
ω_n	undammed natural frequency
ζ	damping ratio

Received: 07 Jul. 2018

Revised: 22 Jan. 2019

Accepted: 09 Mar. 2019

∗Corresponding author:

E-mail: me1816@gmail.com (M. Shahparasti)

Digital object identifier: 10.22098/joape.2019.5015.1381

Research Paper

1. INTRODUCTION

It is anticipated that a major demand for electrical energy will be provided through the installation of renewable energy sources (RESs) due to the economic, technical and environmental issues [1-2]. An inverter is used to transform the power from RESs to the Point of Common Coupling (PCC). The inverter is employed to supply the local load with standard voltage, and to exchange power with the grid. Inverter has two operation modes: grid-connected and stand-alone depending on the grid status [3-4]. In the case of disturbances occurred in the grid voltage, the inverter is disconnected from the grid and the local load is fed in standalone mode [5]. Up to now, many control strategies have been proposed to control inverter current or grid current in grid-connected mode, to control load voltage in standalone mode and to seamless transform between two operation modes [6]. Various standards have been introduced to identify the criteria of load voltage quality and grid current quality [7-8]. The requirements of IEEE 519 standard for the maximum allowed harmonics in the load voltage and IEEE 1547 for grid current are given in Table. 1.

Table 1. IEEE519 for load voltage and IEEE 1547 for grid current.

Individual Harmonic order	$h<11$	$11\leq h<17$	$17\leq h<23$	$23\leq h<35$	$35\leq h$	THD
Grid current (%)	4.0	2.0	1.5	0.6	0.3	5.0
Load voltage (%)	3.0	3.0	3.0	3.0	3.0	5.0

Fig. 1 shows three possible structures of the inverter connected to the local load and grid [7]. The inverter is connected to the grid through the LC and LCL filter as shown in Fig. 1(a) and Fig. 1 (b&c) respectively. Particularly, there are two types of control methods for controlling the inverter which is based on the current control and voltage control [9-10]. For the current control method in the grid-connected mode, the inverter is operated as a controlled current source with a high bandwidth to increase the quality of converter current or grid current [11]. Typically, the purpose of having a current control type is to draw a sinusoidal current from the VSI. If the local load is non-linear and the inverter current is sinusoidal, then the grid current is non-sinusoidal and will be equal to the difference between the inverter current and load current. In Ref. [12], a current-voltage control method is presented based on H^{∞} controller which provides a means to directly control the grid current. Therefore, in Ref. [12] the grid current is always sinusoidal despite the non-linearity of the load. In Ref. [13] a non- sinusoidal current is injected into the PCC to mitigate the harmonic component of the grid current.

Toggling between two working modes leads to smearing a non-standard voltage to the load and receiving an inrush current from the grid [14]. A parallel control system containing a load voltage loop and current grid is proposed in [15] to provide seamless transform. In Refs. [14] and [16] the possibility of a seamless transform between the working modes has been established by designing an appropriate phase locked loop (PLL). A droop control (voltage type control) is another approach that can be considered to control the inverter [17-18]. With an implementation of droop control, it is possible to exchange an active power and reactive power with the grid by controlling the frequency and load voltage amplitude [19-20]. Depending on the grid impedance, the droop method can be implemented in different ways [21]. In Ref. [22], indirect current control for the inverter with LCL filter has been presented. The inverter is possible to operate in two working modes by controlling the amplitude and phase of the capacitor voltage. Indirect current control is related to the droop control method and it is possible to gain a seamless transform between the two working modes. The voltage type control can be enhanced by controlling the inverter to emulate a resistance at the harmonic frequency [23], hence the harmonic current flowing into the grid can be mitigated [24-25].

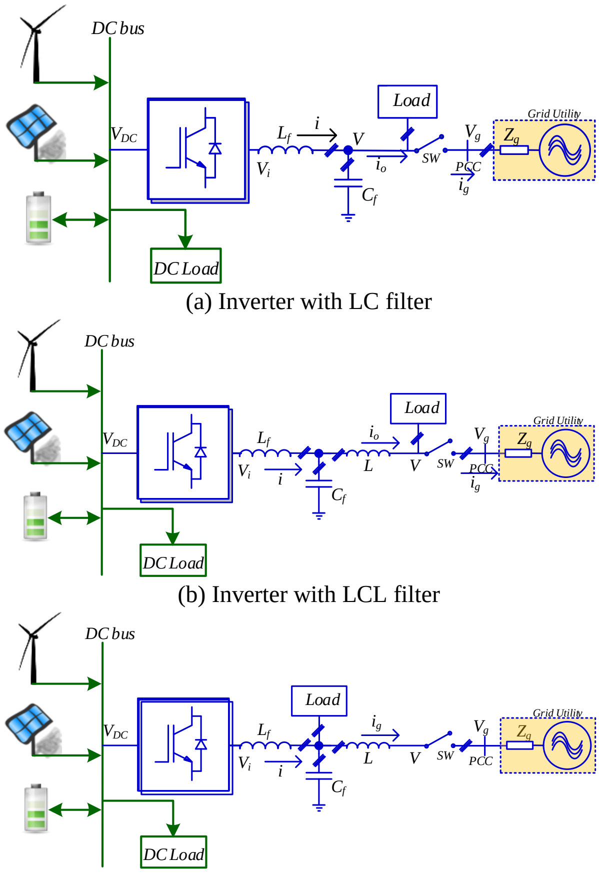

(a) Inverter with LC filter

(b) Inverter with LCL filter

(c)Inverter with LC-L filter

Fig.1. Single line diagram of possible structures of Inverter.

Two important parameters for connecting/disconnecting the inverter to/from the grid is the amplitude and the frequency of the grid voltage. Based on the IEEE 1547 standard, in case of disturbances, the inverter can be disconnected from the grid and feed the load in a stand-alone mode after a specific clearing time. Only the frequency and voltage amplitude have been stated clearly in the standard. Based on the IEEE 1547 standard, if the grid voltage amplitude is between 88% and 110% of the nominal voltage, the inverter has to remain connected to the grid. Also, if the grid voltage is distorted, the inverter should remain connected to the grid. In the grid-connected mode, the existing control strategy is mainly focused on the quality of the grid current or the voltage at the PCC (see load voltage in Fig.1a&b), and improving both of them have not been addressed yet. This paper focuses on grid-connected mode; the main goal is to improve the quality of the grid current and the load voltage under non-ideal grid voltages and non-linear local loads. The main contributions of this paper can be listed as follows:

1) Presenting an adaptive control strategy to determine the voltage waveform of the local load in order to supply the load with a standard voltage under disturbances and also to control the injected current to the grid and exchange the active power to the grid simultaneously.
2) Presenting a cascaded power-voltage-current control structure to implement the proposed control strategy.
3) Critically reviewing and analyzing the performance of the proposed control strategy by comparing the proposed control method with a typical control method.

In order to control the load voltage quality in the grid-connected mode, the load has to be separated from the grid by using impedance. The inductor is the most effective option for such purpose because it does not consume any active power. The equivalent proposed inverter circuit in this study is presented in Fig. 1-c.

The rest of this paper is organized as follows. In sections 2 and 3 the introduction of the proposed control strategy and its implementation are described, respectively. The control parameters selection, simulation results and comparative studies to verify the performance of the proposed control strategy are detailed out in Section 4. The conclusion of the work is presented in Section 5.

2. PROPOSED ADAPTIVE CONTROL STRATEGY

One of the contributions of the paper is the voltage has been let to contain some harmonics (satisfying standards) in order to reduce the grid current harmonics. The way of estimating the voltage and current harmonics and tuning them to some appropriate values by consideration of the voltage conditions and active power reference is another innovation. Implementing such control strategy on a real inverter through a precise simulation is another contribution of the manuscript. Another innovation in the proposed control strategy is the selection of load voltage waveform (V) which should be obtained from the inverter in stand-alone and grid-connected modes.

In the stand-alone mode, the load voltage reference is a pure sinusoidal voltage. However, in order to explore the proposed strategy for the grid-connected mode, the grid voltage is assumed to have odd harmonics of 5, 7, 11, 13 … as described in (1).

$$\begin{aligned} &V_g(t)=V_{g1}\sin(\omega t)+\\ &V_{g5}\sin(5\omega t+\varphi_5)+\\ &V_{g7}\sin(7\omega t+\varphi_7)+\dots \end{aligned} \tag{1}$$

The load voltage reference can be defined in (2). The load voltage reference is needed to control the quality of load voltage, grid current and power injected to the grid, simultaneously

$$\begin{aligned} &V^*(t)=V_{1n}\sin(\omega t+\delta)\\ &+V_{5n}\sin(5\omega t+\varphi_5)\\ &+V_{7n}\sin(7\omega t+\varphi_7)+\dots \end{aligned} \tag{2}$$

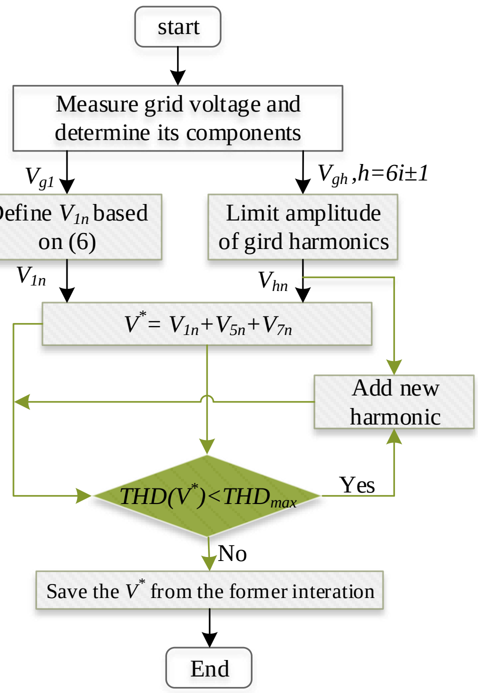

Fig. 2. Flowchart of the proposed method to generate load voltage reference for reducing harmonics of current injected to the grid.

where the load voltage phase (δ) and amplitude voltage n indicates the nominal value. For example V_{1n} is the nominal or maximum allowable value of the fundamental harmonic of the voltage, (V_{1n}) is calculated based on the active and reactive power reference exchanged with the grid. For the h^{th} component of load voltage, the amplitude of the voltage can be denoted as V_h. The amplitude of the h^{th} harmonic of grid current in the grid-connected mode is equal to (3).

$$I_{gh}=\frac{V_h-V_{gh}}{jh2\pi fL} \tag{3}$$

For sensitive load case, the load voltage reference is pure sinusoidal and the grid current in (3) will become non-sinusoidal hence the h^{th} harmonic amplitude of grid current is equal to (4).

$$I_{gh}=\frac{-V_{gh}}{jh2\pi fL} \tag{4}$$

In the proposed adaptive control strategy, an addition of the allowable level of grid voltage harmonics to the load voltage reduces harmonic contents of grid current. The load voltage harmonics are precisely in phase with the grid voltage harmonics in Eq. (2), but their amplitudes are equal to the values given in the standards as shown in Table. I. The first priority of the control strategy is to feed the load with a standard voltage and taking an advantage of the load voltage standard harmonics to eliminate the current harmonics as described in Eq. (5).

$$\begin{cases} Hf_h = \dfrac{V_h}{V_1} \le Hf\,(max) \\ THD_v \le THD_{max} \end{cases} \tag{5}$$

where Hf is the harmonic factor which should be lower than 3% and the THD of voltage THD_v should be lower than 5%. In section 3, the implementation of proposed control strategy will be discussed. For example, based on the flowchart of Fig.2, the maximum available harmonics of grid voltage are added to the load voltage reference to reduce harmonics of the current injected to the grid.

3. IMPLEMENTATION OF PROPOSED CONTROL STRATEGY

The block diagram of the proposed control strategy implementation for the inverter with the LC-L filter is shown in Fig. 3. The implementation of the proposed control strategy is based on the cascaded power-voltage-current control structure in the stationary reference frame. The objective of the proposed control strategy is to perform a significant control of the load voltage, grid current as well as the active power exchanged with the grid.

3.1. Cascaded power-voltage-current control structure

As shown in Fig. 3, the load voltage as well as the grid voltage has been used in the power loop to calculate the power exchange with the grid. The difference between the reference power and the calculated power will pass through power controller. The power controller is an integral controller and m is its coefficient. The output of the power controller is equal to the load voltage phase (δ). The voltage reference in the grid fundamental frequency is built based on the PLL output and the load voltage phase (δ) as described in Eq. (6).

$$\begin{cases} \delta = \dfrac{m}{s}(P^* - P) = m\displaystyle\int (P^* - P)\,dt \\ V_{\alpha 1}^* = V_{1n}\cos(\theta + \delta) \\ V_{\beta 1}^* = V_{1n}\sin(\theta + \delta) \end{cases} \tag{6}$$

Since the load voltage reference is built based on the grid voltage harmonics and the voltage reference in the fundamental frequency, linearizing the power relationship around the operating point ($\delta = \delta_0$) yields:

$$P = \frac{3V_1V_{g1}}{2\pi fL}\sin\delta$$
$$\rightarrow \Delta P = \frac{3V_1V_{g1}}{2\pi fL}\cos\delta_0\Delta\delta = K_s\Delta\delta \tag{7}$$

where K_s is the synchronization coefficient. The inverter is stable when the value of K_s is positive. The block diagram of power loop based on Eq. (7) is shown in Fig. 4-a, where the ω_c is the cutoff frequency of the low pass filter and H_p is the power feedback gain. The closed loop equation of the power loop is given in Eq. (8).

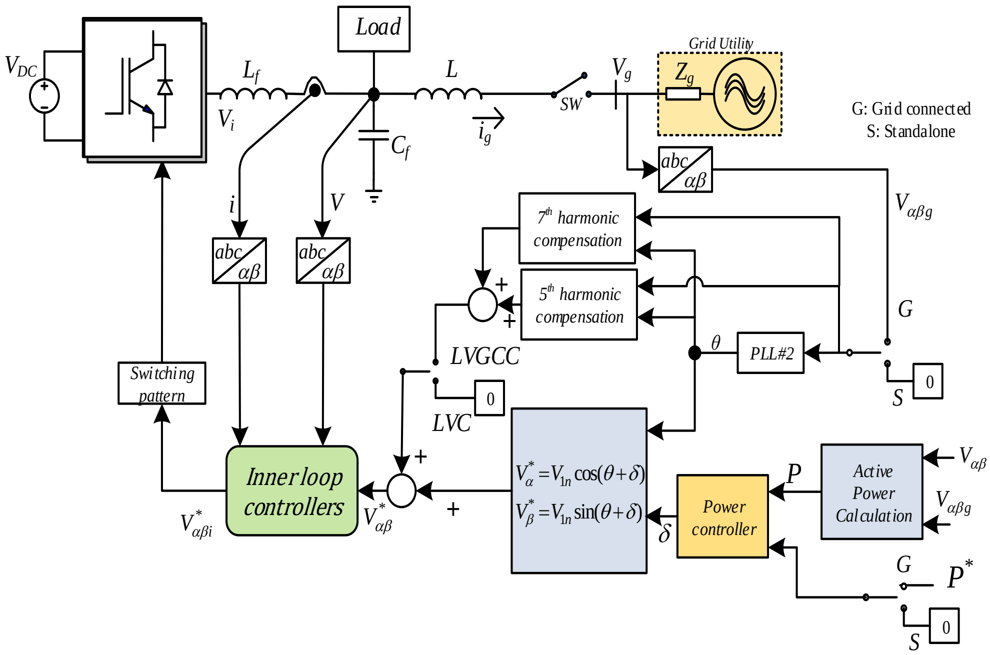

Fig. 3. Proposed inverter with LC-L filter: circuit diagram and implementation of the proposed control strategy.

$$\frac{P}{P^*}=\frac{m.K_s.\omega_c}{s^2+s\omega_c+H_p.m.K_s.\omega_c} \tag{8}$$

Compared to standard two order standard characteristic equation, $s^2+2\zeta\omega_n s+\omega_n^2$ [26], the undamped natural frequency (ω_n) and the damping ratio (ζ) can be controlled by properly tuning the ω_c and m:

$$\omega_n=\sqrt{H_p.m.K_s.\omega_c}$$

$$\zeta=0.5\sqrt{\frac{\omega_c}{H_p.m.K_s}} \tag{9}$$

The main element to be considered in selecting ω_n and ζ are the power loop settling time (T_{sp}). According to the standards, if the maximum deviation of frequency is Δf, the T_{sp} can be defined in Eq. (10).

$$T_{sp}\geq\frac{\delta}{2\pi\Delta f} \tag{10}$$

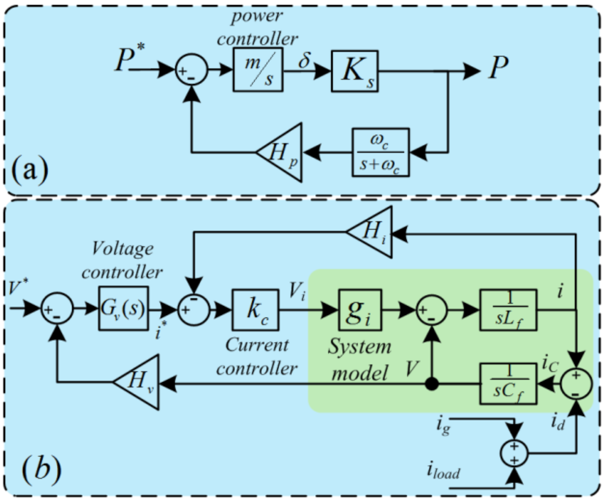

Fig. 4. (a) Power loop. (b) Inner loops for tracking of voltage reference in proposed inverter with LC-L filter in the stationary reference frame.

The inner loop control for tracking the voltage reference is comprising of the current controller as well as the voltage controller as shown in Fig. 4-b. For design consideration of controllers, separating the current and voltage loop is one of the most desirable methods. The proposed inverter in the stationary reference frame ($\alpha\beta$) can be expressed in Eq. (11) for both grid-connected and stand-alone modes [27-28].

$$\begin{cases}\dfrac{di}{dt}=\dfrac{v_i-v}{L_f}\\[2ex]\dfrac{dv}{dt}=\dfrac{i-i_g-i_{load}}{C_f}=\dfrac{i-i_d}{C_f}\end{cases} \tag{11}$$

When the disturbance input (i_d) is ignored, the system model transfer function is given by (12).

$$\frac{i_L(s)}{V_i(s)}=\frac{sg_iC_f}{1+s^2L_fC_f} \tag{12}$$

However, this system is unstable and susceptible to resonance oscillation. This condition can be overcome by using a proportional controller in the current control loop ($G_i(s)=k_c$), where the closed loop function can be described in Eq. (13).

$$\frac{i(s)}{i^*(s)}=\frac{sg_ik_cC_f}{1+sg_iH_ik_cC_f+s^2L_fC_f} \tag{13}$$

A better damping of resonance oscillation as well as a good tracking speed of the reference current can be achieved by increasing the value of k_c. However, the stability limit must be taken into account when increasing the value of k_c. Over tuning the value of k_c could leads to the generation of high-order harmonics and instability. Therefore, the value of k_c must be chosen properly as to maintain a good performance of the current control.

According to the proposed control strategy, the voltage controller has to be able to track a voltage reference which consisting of the fundamental frequency and its odd-harmonic frequencies. However, when disturbances due to the load current and grid voltage occurred, it is quite difficult for the voltage controller to follow the voltage reference. Thus, a new voltage controller with the following transfer function is proposed in the voltage loop.

$$G_v(s)=\left(k_{p1}+{k_{i1}}/{s}\right)\left(\frac{\pi^2}{4}-\frac{\pi\omega_e}{2s}\tanh\left(\frac{\pi s}{2\omega_e}\right)\right) \tag{14}$$

The proposed voltage controller is implemented with the least extent of calculations in the stationary reference frame with a capability of tracking the harmonics. A derivation of a voltage controller from the synchronous reference frame proportional–integral multi-loop controller including its parameters design and evaluation has been published in Ref. [29]. The controlling parameters of the proposed voltage controller have been chosen based on the bandwidth, phase margin and odd harmonic gains correspond to the open loop system response.

3.2. PLL and synchronism with grid

Two PLLs have been considered to synchronize the inverter with the grid and to produce a voltage reference signal. The PLL#1 input is a per unit voltage in a stationary reference frame that produces the voltage amplitude (V_d), frequency (f) and voltage phase (θ) [30]. In the case of the grid outage, the PLL#2 produces angle for generating sinusoidal voltage reference with a base frequency and the inverter will work in stand-alone mode to feed the local load. When the grid returns to its normal condition, the inverter has to switch back to the grid-connected mode by going through the synchronization procedure. Fig. 5 demonstrates the proposed logic scheme behind this idea for synchronizing with the grid where the frequency and the grid voltage amplitude are initially extracted from PLL#1, the command for connecting the system back to the grid is according to the IEEE 1547 standard limits. As shown in Fig. 5, the grid voltage is applied to the PLL#1 and the inverter voltage reference will be equal to the grid voltage. As soon as the difference between the grid voltage and the load voltage becomes less than a certain amount (eV_{max}), a closing command is released for the SW circuit breaker.

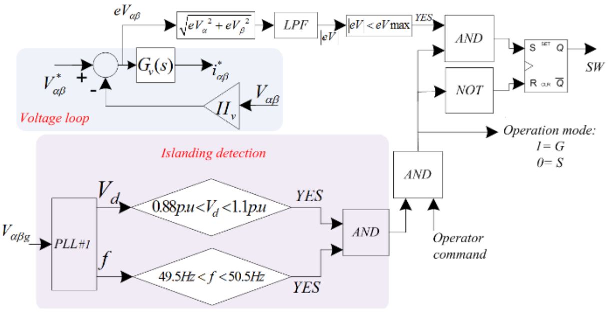

Fig. 5. Proposed logic scheme for connection to the grid and disconnection from the grid.

3.3. Elimination of grid current harmonics

Based on Eq. (2), the harmonics of injected current to the grid is obtained due to the differences between the grid voltage and the load voltage in various frequencies. The dominant harmonics of grid voltage relies on the odd harmonics of 5, 7, 11, 13 and etc which results in the flowing of harmonic currents between the grid and the PCC. In proposed strategy, the idea of adding a suitable harmonic voltage to the load voltage reference is proposed for the restriction of current harmonic amplitudes of 5th and 7th. The maximum load voltage reference harmonic parameters and its relative THD in the grid-connected mode are equal to 3% and 5% respectively. In compensation blocks of 5th and 7th harmonics as shown in Fig. 3, the harmonics component of grid voltage is extracted and the permissible amount is added to the voltage reference obtained in (6). When the load voltage has exactly the same harmonics content as grid voltage, the amount of current harmonics is reduced according to Eq. (3). Thus, by choosing the correct size of the inductor, harmonics with the higher order than 11th can be restricted and the interface inductor should be in the range given in Eq. (15) where the δ_{max} is the maximum angle difference between the load voltage and the grid which is normally less than 40°. By referring to Eq. (15), P_n and $V_{g11,max}$ are the nominal power exchange with the grid and the maximum content of 11th grid voltage harmonic respectively.

$$\frac{V_{g11}}{22\pi f} < L < \frac{3V^2}{2\pi f P_n} sin(\delta_{max}) \tag{15}$$

4. Design, simulation and evaluation

To validate the efficiency of the proposed control strategy, the inverter connected to the grid through the LC-L filter is simulated by the parameters given in Table II. In the simulation, the grid voltage is considered with 5% of 5th harmonics and 4% of 7th harmonics. The local load of inverter includes a 10 kW non-linear load and a 4 kW linear load at 0.8 lagging power factor. In order to make a proper assessment of the conventional inverters reviewed in the introduction, the inverter with LCL filter and current type controller introduced in Ref. [3] will also be simulated. The parameters of the inverter with LCL filter are completely similar to the data presented in Table. 2.

4.1. Control Parameters Selection

In the simulation for the power controller, m=7.5 is used in order to get a good compromise in the settling time and overshoot. The step response of power loop is shown in Fig. 6-a where it can be seen that the settling time is 0.11s and the overshoot is about 1%, respectively. Based on the discussion stated in the previous section and Ref. [27], the value of k_c=2.5 is selected for the current loop. The proportional factor of the proposed voltage controller (k_{p1}) in the voltage loop given in Ref. [27] is chosen according to the bandwidth and phase margin of open loop response. The integral factor is set based on the proportional factor and nominal system parameters ($k_{i1}=k_{p1}/RC$). For k_{p1}=0.8 and k_{i1}=2000, the open loop response of the system is shown in Fig. 6-b where the gain in odd harmonics is more than 40 db which kept the steady state error less than 1%.

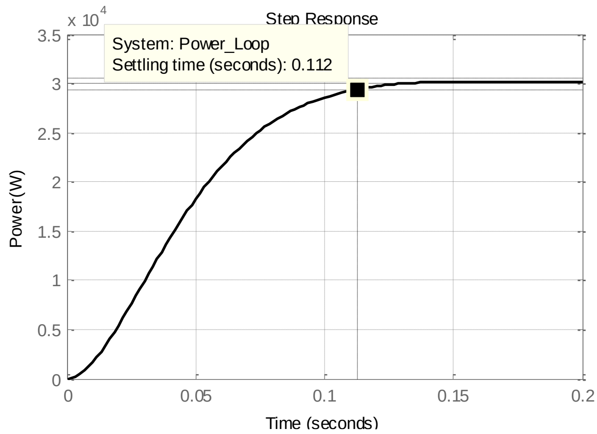

(a)

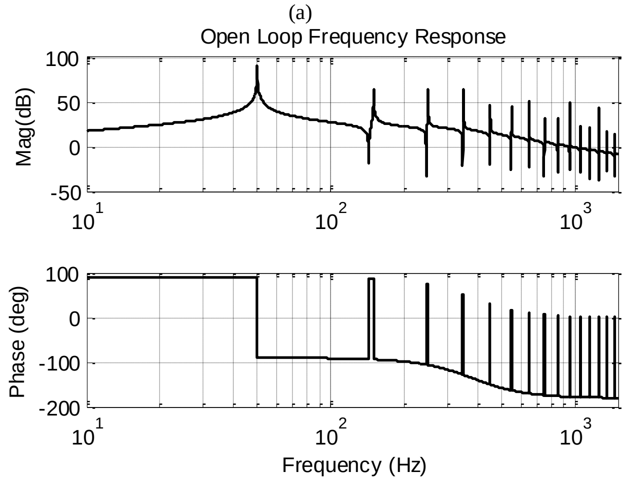

(b)

Fig. 6. Inverter with LC-L filter. (a) power loop (b) open loop response for voltage loop.

Table 2. Inverter with LC-L filter parameters

Description	Symbol	Value
Filter inductance	$L_f + rL$	2.87 mH+0.05 Ω
Filter capacitor	C_f	60 µF
Interface inductance	L	2 mH + 0.3 Ω
Switching frequency	f_s	10 kHz
Grid voltage	$V_{abc,g}$	380 V
Grid Frequency	f	50 Hz
Inverter DC voltage	V_{DC}	700 V

4.2. Time domain analysis

A comparative study between the inverter with LC-L filter and inverter with LCL filter is discussed in this subsection. In the grid-connected mode, the main signals to compare the two mentioned structures are particularly relies on the load voltage, grid current, inverter current and the exchanged of active and reactive power.

The simulation results of the inverter with LCL filter in the grid-connected mode are shown in Fig. 7(a). In this structure, the main objective is to draw a sinusoidal current with a unity power factor from the inverter. The result shows that the control design presented in [3] has covered this purpose. However, this is totally depending on the types of the load, the preference of the inverter and the grid connection. If the inverter current is sinusoidal and the load current is non-sinusoidal, then the grid current will be non-sinusoidal and unable to achieve a unity power factor. To have a better vision of this fact, the load voltage harmonic spectrum (grid voltage) and grid current are demonstrated in Figs. 8(a)&(b). It can be seen that, even though the inverter current is sinusoidal with a THD lower than 1.97%, the grid current is non-sinusoidal with a THD of 7.84%.

The simulation results of the proposed strategy for the inverter with LC-L filter are illustrated in Figs. 7 (b&c). As stated in the introduction, the main purpose of this strategy is to supply the load in a standard voltage with an independent of grid voltage status. When the V_{1n} is set to 1p.u, the reactive power is not controllable. The simulation results for V_{1n}=1p.u and $V_{5n}=V_{7n}=0$ are presented in Fig. 7(b). The harmonic spectrum of the load voltage and the grid current are presented in Figs. 8 (c&d) respectively. Despite the distortion of the grid voltage (THD about 6.47%) and the non-linearity of the load (THD 11.12%), the load is fed with a standard sinusoidal voltage of THD=1.66%. The harmonic spectrum of grid current is given in Fig. 8(d) where the harmonics are independent from the load current harmonics and are dependent on grid voltage harmonics. Since the compensation of harmonics in the grid current is not an objective, therefore the THD content and harmonic amplitudes of grid current are out of the standard limit. By comparing the harmonic spectrums of the load current

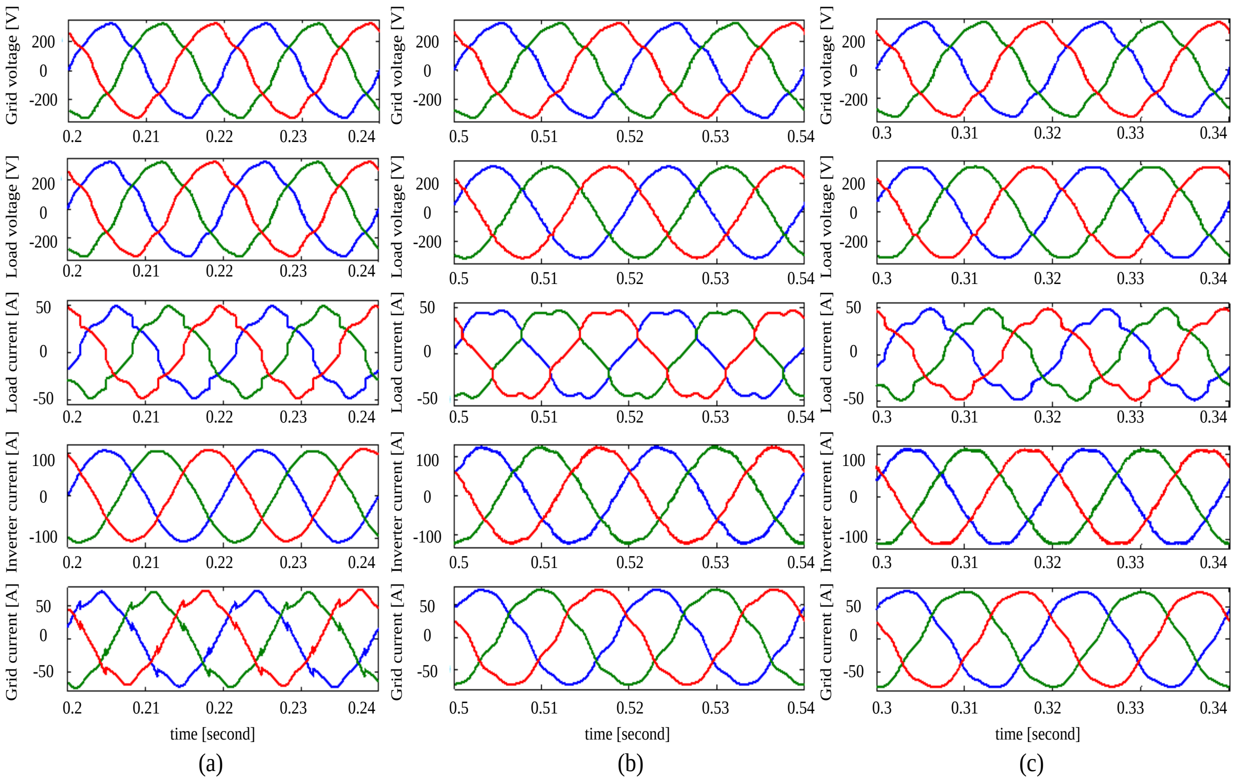

Fig. 7. Simulation results for the grid-connected mode: (a) Inverter with LCL filter (common structure), (b) Inverter with LC-L filter and with "V_{1n}=1p.u, $V_{5n}=V_{7n}$=0 reference voltage", (c) Inverter with LC-L filter and with "V_{1n}=1p.u, $V_{5n}=V_{7n}$=0.03p.u reference voltage". From down: grid current, inverter current, load current, load voltage, grid voltage.

with the inverter current and the grid current, it can be concluded that the differences between the current harmonics of the load and the grid are supplied by the inverter.

For the case of V_{1n}=1p.u and V_{5n}=V_{7n}=0.03p.u, the simulation result as well as the harmonic spectrum is given in Fig. 7(c) and Fig. 8(e&f) respectively. It can be seen that, by adding 5th and 7th harmonics to load voltage, the quality of current injected to the grid has improved in comparison with the case of V_{1n}=1p.u, V_{5n}=V_{7n}=0 and the THD of grid current has been decreased from 6.47% to 4.41%. It should be noticed that the improvement in the

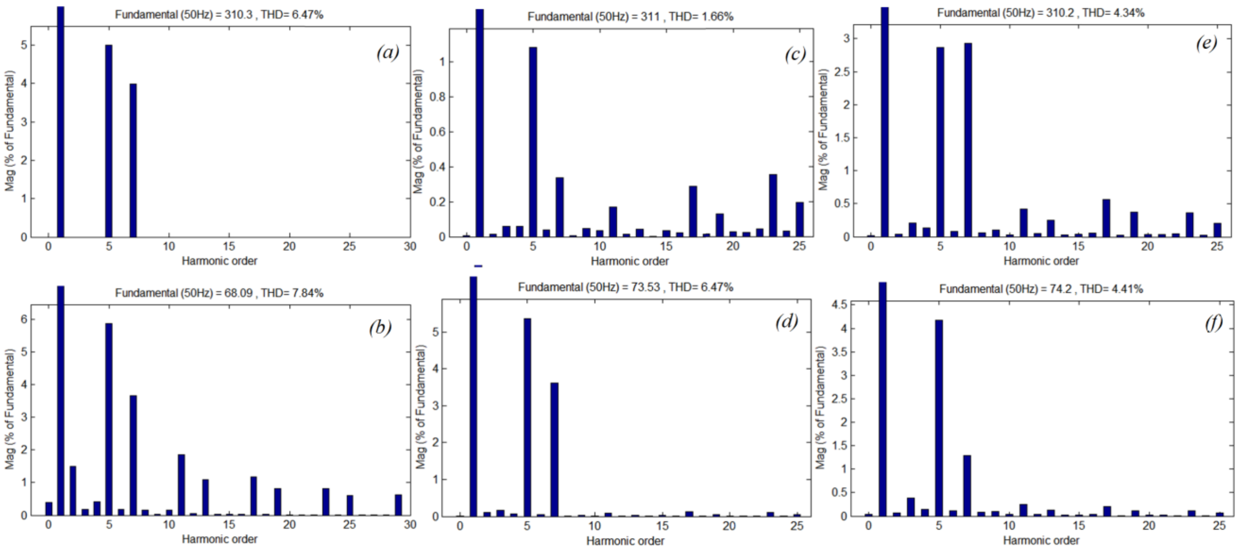

Fig. 8. Fourier spectrum of the simulation results for the grid-connected mode:
a) Grid voltage and load voltage in inverter with LCL filter (common structure).
b) Grid current in inverter with LCL filter (common structure).
c) Load voltage in inverter with LC-L filter for the case of V_{1n}=1p.u and V_{5n}=V_{7n}=0 reference voltage.
d) Grid current in inverter with LC-L filter for the case of V_{1n}=1p.u and V_{5n}=V_{7n}=0 reference voltage.
e) Load voltage in inverter with LC-L filter for the case of V_{1n}=1p.u and V_{5n}=V_{7n}=0.03p.u reference voltage.
f) Grid current in inverter with LC-L filter for the case of V_{1n}=1p.u and V_{5n}=V_{7n}=0.03p.u reference voltage.

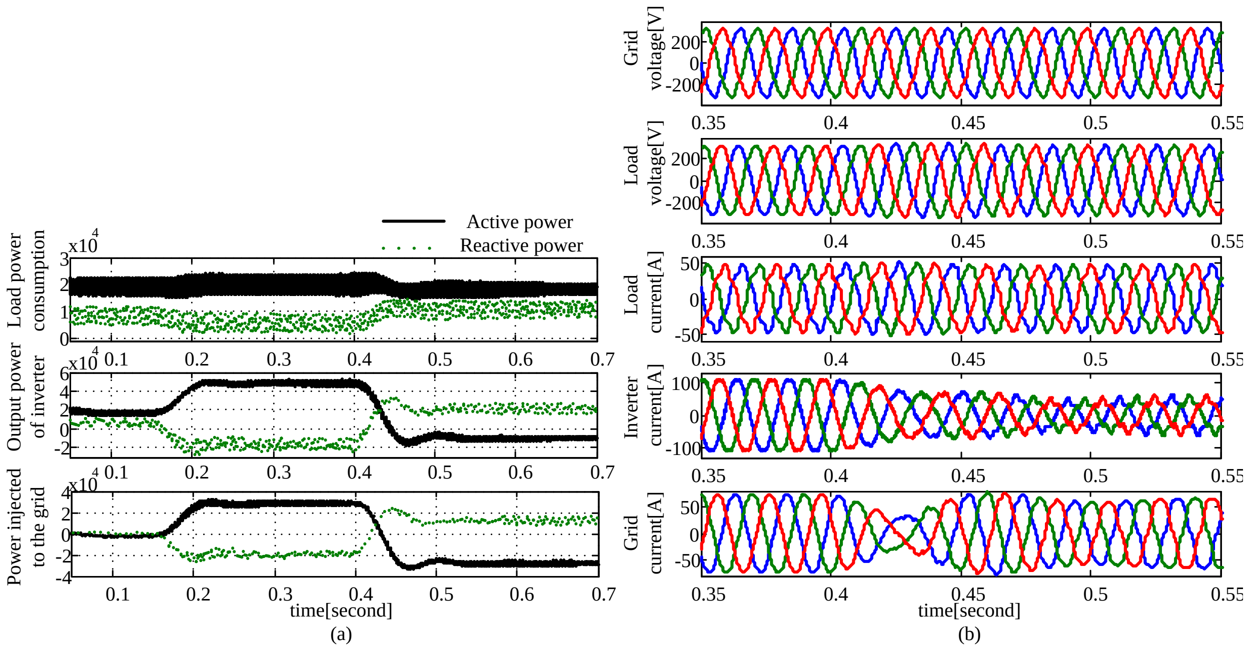

Fig. 10. Inverter with LC-L filter. A simulation results of power reference step change. (a) From down: power injected to the grid, inverter power, load power. The active and reactive power at the load, inverter and grid. (b) From down: The waveforms of the grid current, inverter current, load current, load voltage and grid voltage.

quality of the grid current has a significant contribution in a quality reduction of load voltage.

The simulation results of switching from the stand-alone mode to the grid-connected mode and vice versa are shown in Fig. 9. In an ideal condition, the interchange between the two operation modes should not affect the quality of local load voltage. In Fig. 9, there are three intervals: startup, grid-connected and standalone.

In startup interval, it is assumed that at t=0s the command for connection to the grid is released by the operator. The inverter starts with working in standalone mode and tries to supply the load with the same voltage of grid. As it can be seen from Fig.9 to reduce initial current of inverter and load, inverter supplies load with 10% of nominal voltage and amplitude of inverter voltage increase from 0.1p.u. until 1 p.u. with the specific rate. Consequently, the inverter tries to equalize the load voltage and the grid in terms of sequence, amplitude and phase through the internal controllers while the active power reference is set to zero. As soon as the difference between the load voltage and the grid voltage drop to a certain amount, the circuit breaker will connect the inverter to the grid. In this simulation, the process takes place at t=0.058s where the inverter connects to the grid. In grid-connected mode, the inverter can inject power to the grid. At t=0.18 second, the power reference changes from 0 to 50kW. It can be seen that the reference power is tracked after 20ms with zero steady state error without overshoot. The inverter will exchange the power with the grid until t=0.4s. At t=0.4s, a disconnection command from the grid is released by the operator and the circuit breaker is opened and the inverter supplies the local load in a stand-alone mode.

According to the optimal operation scheduling of microgrids, it is required to inject or receive power to or from the grid. The active reference power changes from 30kW to -30kW at t=0.4s as shown in Fig. 10. In Fig. 10(a), the power reference is tracked in 0.1s and the reference power is precisely injected to the grid. Additionally, Fig. 10(b) shows that changing amount of exchanged power with the grid has no effect on the quality of the load and the load is fed with a completely standard voltage.

The final simulations are done to examine the system performance operating under weak grid voltage conditions. The short circuit capacity (SCC) in amps (A) is equal to the nominal grid voltage in volts (V) divided by the grid equivalent impedance *Zg* in ohms (Ω). In this paper, to evaluate the system performance in the worst case, the proposed system is connected to grid with SCC from 2.5kA until 15kA. Other conditions of simulation are the same as previous ones. Figs 11&12 show the summary of several simulations as 2 graphs where THD and percentage of fifth and seventh harmonics (H_{f5} and H_{f7}) are used as criteria to evaluate the results.

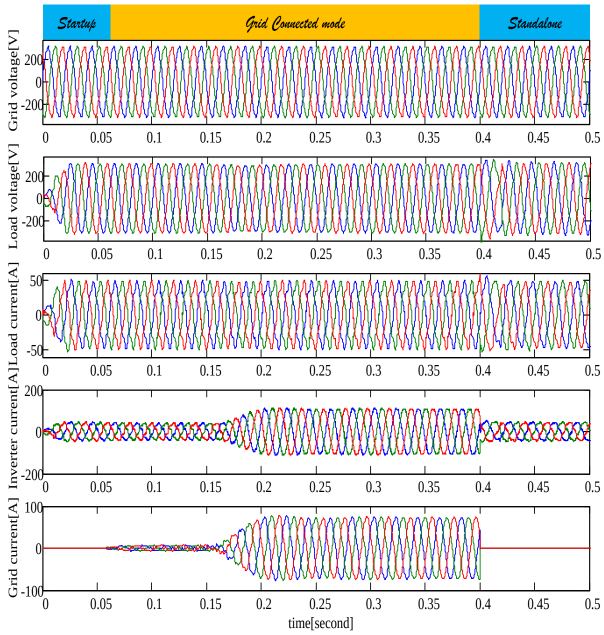

Fig. 9. Simulation results of switching between two operation modes. From down: grid current, inverter current, load current, load voltage and grid voltage.

Other conditions of simulation are the same as previous ones. Figs 11&12 show the summary of several simulations as 2 graphs where THD and percentage of fifth and seventh harmonics (H_{f5} and H_{f7}) are used as criteria to evaluate the results. The main important point that the systems work properly in all of SCCs is due to the suitable design of controllers. Fig. 11 shows H_{f5}, H_{f7} and *THD* of load voltage. It can be seen that H_{f5}, H_{f7} and *THD* of load voltage and PCC voltage are the same for the inverter with LCL filter in of SCCs and their values are out of standard ranges. For inverter with LC-L filter in the case of V_{1n}=1p.u and V_{5n}=V_{7n}=0 reference voltage, the load voltage is controlled independently of grid voltage in all of SCCs where values of H_{f5}, H_{f7} and *THD* for load voltage are about 1.1%, 0.2% and 1.7%, respectively. Also, for voltage reference with V_{1n}=1p.u and V_{5n}=V_{7n}=0.03p.u, values of H_{f5}, H_{f7} and *THD* of load voltage are lower than 3%, 3% and 4%, respectively. For current injected to the grid in Fig.12, the inverter with LC-L filter in the case of V_{1n}=1p.u and V_{5n}=V_{7n}=0.03p.u reference voltage can keep the quality of i_g in the standard range for all of SCCs. The inverter with LCL filter, the H_{f5}, H_{f7} and *THD* of i_g are far from standards. Also, the inverter with LC-L filter in the case of V_{1n}=1p.u and V_{5n}=V_{7n}=0.03 reference voltage cannot control the quality of i_g in standard range. From these graphs, it can be concluded that the proposed configuration with related control strategy works properly in different SCCs.

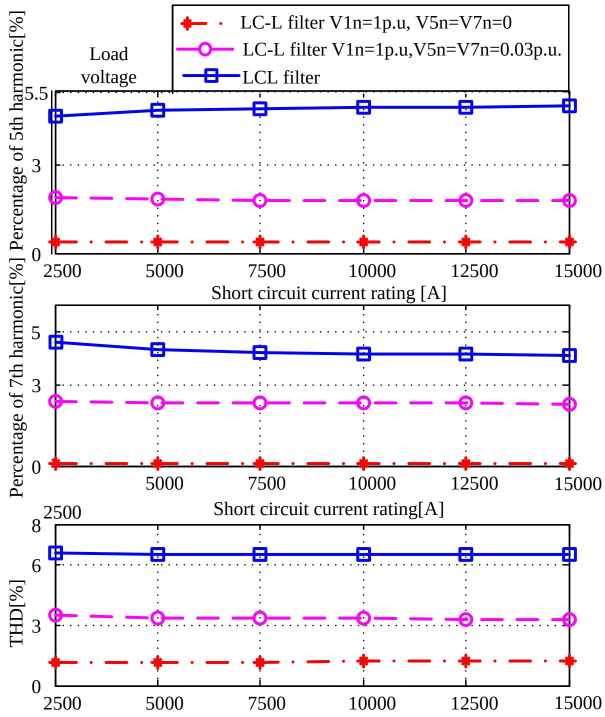

Fig. 11: Simulation results of load voltage for the grid-connected mode. From up: Percentage of fifth harmonic, Percentage of seventh harmonic and THD.

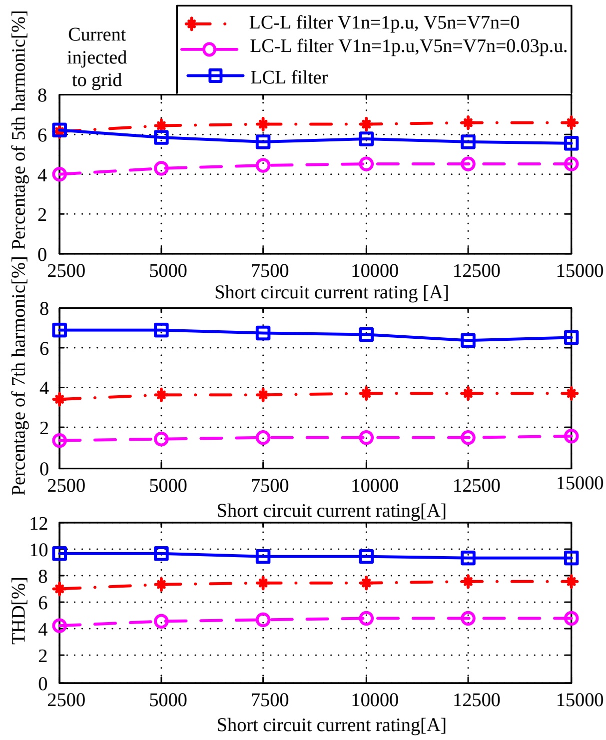

Fig. 12: Simulation results of current injected to grid for the grid-connected mode. From up: Percentage of fifth harmonic, Percentage of seventh harmonic and THD.

5. Conclusion

In conventional structures of the inverter, the load is connected to the grid directly without any intermediate impedance. Thus, the distortions of grid voltage will be applied to the load directly and it is not possible to feed the load in a standard quality of service. To resolve this problem and to ensure that the load is feed in an appropriate quality, an inverter with LC-L filter has been proposed where an inductor is used as an interface between the grid and the local load. An adaptive strategy is proposed to simultaneously control the load voltage and grid current. The proposed control strategy is able to control the harmonics of the current injected to the grid by purposely reducing the quality of load voltage. The inverter with LC-L filter is accurately modeled and a control scheme with a three loop of power-voltage-current has been introduced for the implementation of the proposed strategy. A comparative study between the inverter with LC-L filter and the conventional inverter structure with LCL filter from various perspectives has been carried out. Based on the simulation results, it has been shown that the proposed inverter perform suitably in maintaining the quality of load voltage and current injected to the grid.

Acknowledgement

The authors are thankful to authorities of East Tehran Branch, Islamic Azad University, Tehran, Iran, for providing support and necessary facilities

REFERENCES

[1] R. Esmaeilzadeh, A. Ajami, and M. R. Banaei, "Two-Stage Inverter Based on Combination of High Gain DC-DC Converter and Five-Level Inverter for PV-Battery Energy Conversion," *J. Oper. Autom. Power Eng.*, vol. 6, no. 1, pp. 101–110, 2018.

[2] M. A. Hassas and K. Pourhossein, "Control and Management of Hybrid Renewable Energy Systems : Review and Comparison of Methods," *J. Oper. Autom. Power Eng.*, vol. 5, no. 2, pp. 131–138, 2017.

[3] M. Abbasi and B. Tousi, "A Novel Controller Based on Single-Phase Instantaneous p-q Power Theory for a Cascaded PWM Transformerless STATCOM for Voltage Regulation," *J. Oper. Autom. Power Eng.*, vol. 6, no. 1, pp. 80–88, 2018.

[4] H. Moayedirad and M. A. S. Nejad, "Increasing the Efficiency of the Power Electronic Converter for a Proposed Dual Stator Winding Squirrel-Cage Induction Motor Drive Using a Five-Leg Inverter at Low Speeds," *J. Oper. Autom. Power Eng.*, vol. 6, no. 1, pp. 23–39, 2018.

[5] R. Ghanizadeh, M. Ebadian, and G. B. Gharehpetian, "Control of Inverter-Interfaced Distributed Generation Units for Voltage and Current Harmonics Compensation in Grid- Connected Microgrids," *J. Oper. Autom. Power Eng.*, vol. 4, no. 1, pp. 66–82, 2016.

[6] Allal M. Bouzid, Josep M. Guerrero, Ahmed Cheriti, Mohamed Bouhamida, Pierre Sicard, Mustapha Benghanem, A survey on control of electric power distributed generation systems for microgrid applications, *Renew. Sustain. Energy Rev.*, vol. 44, 2015, pp. 751-766, 2015.

[7] IEEE Draft "Standard for Interconnection and Interoperability of Distributed Energy Resources with Associated Electric Power Systems Interfaces," *IEEE P1547/D7.0*, September 2017 , pp.1-147, 2017.

[8] "IEEE Recommended Practices and Requirements for Harmonic Control in Electrical Power Systems," *IEEE Std* 519-1992 , pp.1-112, April 9 1993
[9] J. Rocabert, A. Luna, F. Blaabjerg, and P. Rodríguez, "Control of power converters in AC microgrids," *IEEE Trans. Power Electron.*, vol. 27, no. 11, pp. 4734–4749, 2012.
[10] M. Heidari and M. Monfared, "A New Control Method for Single-Phase Grid-Connected Inverter Using Instantaneous Power Theory," *J. Oper. Autom. Power Eng.*, vol. 5, no. 2, pp. 105–116, 2017.
[11] M. Shahparasti, P. Catalán, J. I. Candela, A. Luna and P. Rodríguez, "Advanced control of a high power converter connected to a weak grid," *IEEE Energy Convers. Congress Exposition (ECCE)*, Milwaukee, WI, 2016, pp. 1-7.
[12] Q. Zhong and T. Hornik, "Cascaded Current – Voltage Control to Improve the Power Quality for a Grid-Connected Inverter With a Local Load," *IEEE Trans. Ind. Electron.*, vol. 60, no. 4, pp. 1344–1355, 2013.
[13] M. Cirrincione, M. Pucci, and G. Vitale, "A single-phase DG generation unit with shunt active power filter capability by adaptive neural filtering," *IEEE Trans. Ind. Electron.*, vol. 55, no. 5, pp. 2093–2110, 2008.
[14] T. V. Tran, T.-W. Chun, "PLL-Based Seamless Transfer Control Between Grid-Connected and Islanding Modes in Grid-Connected Inverters," *IEEE Trans. Power Electron.*, vol. 29, pp. 5218-5228, 2013.
[15] M. Arafat and S. Palle, "Transition control strategy between standalone and grid-connected operations of voltage-source inverters," *IEEE Trans. Power Electron.*, vol. 48, no. 5, pp. 1516–1525, 2012.
[16] D. S. Ochs and B. Mirafzal, "A Method of Seamless Transitions Between Grid- Tied and Stand-Alone Modes of Operation for Utility-Interactive Three-Phase Inverters," *IEEE Trans. Power Electron*., vol. 50, pp. 1934-1941, 2013.
[17] U. B. Tayab, M. A. B. Roslan, L. J. Hwai, M. Kashif, "A review of droop control techniques for microgrid," *Renew. Sustain. Energy Rev.*, vol. 76, pp. 717-727, 2017.
[18] S. M. Azimi, S. Afsharnia, "Multi-purpose droop controllers incorporating a passivity-based stabilizer for unified control of electronically interfaced distributed generators including primary source dynamics," *ISA Trans.*, vol. 63, pp. 140-153, 2016.
[19] A. Urtasun, P. Sanchis, L. Marroyo, "State-of-charge-based droop control for stand-alone AC supply systems with distributed energy storage," *Energy Convers. Manage.*, vol. 106, pp. 709-720, 2015
[20] M. A. Ghasemi, M. Parniani, "Prevention of distribution network overvoltage by adaptive droop-based active and reactive power control of PV systems," *Electr. Power Syst. Res.*, vol. 133, pp. 313-327, 2016.
[21] V. Mortezapour, H.Lesani, "Hybrid AC/DC microgrids: A generalized approach for autonomous droop-based primary control in islanded operations," *Int. J. Electr. Power Energy Syst.*, vol. 93, pp. 109-118, 2017.
[22] J. Kwon, S. Yoon, and S. Choi, "Indirect current control for seamless transfer of three-phase utility interactive inverters," *IEEE Trans. Power Electron.*, vol. 27, no. 2, pp. 773-781, 2012.
[23] J. He, Y. W. Li, and M. S. Munir, "A flexible harmonic control approach through voltage-controlled DG-grid interfacing converters," *IEEE Trans. Ind. Electron.*, vol. 59, no. 1, pp. 444–455, 2012.
[24] [24] H. Zhang; S. Kim; Q. Sun; J. Zhou, "Distributed Adaptive Virtual Impedance Control for Accurate Reactive Power Sharing Based on Consensus Control in Microgrids," *IEEE Trans. Smart Grid*., vol. 8, pp.1749-1761, 2017.
[25] M. A. Abusara, M. Josep, "Improved droop control strategy for grid-connected inverters," *Sustain. Energy, Grids Networks*, vol. 1, pp. 10-19, 2015.
[26] Ka. Ogata, "Modern Control Engineering," *Prentice Hall*, 2010.
[27] D. N. Zmood and D. G. Holmes, "Stationary frame current regulation of PWM inverters with zero steady-state error," *IEEE Trans. Power Electron.*, vol. 18, no. 3, pp. 814–822, 2003.
[28] C. Zou, B. Liu, S. Duan, and R. Li, "Stationary Frame Equivalent Model of Proportional-Integral Controller in dq Synchronous Frame," *IEEE Trans. Power Electron.*, vol. 29, no. 9, pp. 4461–4465, 2014.
[29] M. Shahparasti, M. Mohamadian, A. Yazdian, A. Ale Ahmad and M. Amini "Derivation of a Stationary-Frame Single Loop Controller for Three Phase Standalone Inverter Supplying Nonlinear Loads," *IEEE Trans. Power Electron.*, vol. 29, no. 9, pp. 5063- 5071, 2014.
[30] K. H. Ahmed, A. M. Massoud, S. J. Finney, and B. W. Williams, "Sensorless Current Control of Three-Phase Inverter-Based Distributed Generation," *IEEE Trans. Power Del.*, vol. 24, no. 2, pp. 919–929, 2009.